

Relevance of multiband Jahn-Teller effects on the electron-phonon interaction in  $A_3C_{60}$ E. Cappelletti<sup>1,2</sup>, P. Paci<sup>2</sup>, C. Grimaldi<sup>3</sup> and L. Pietronero<sup>2</sup><sup>1</sup>\Enrico Fermi" Research Center, c/o Compendio del Viminale, v. Panisperna 89/a, 00184 Roma, Italy<sup>2</sup>Dipart. di Fisica, Universita "La Sapienza", P.le A. Moro, 2, 00185 Roma, and INFN RM1, Italy and<sup>3</sup>Ecole Polytechnique Fédérale de Lausanne, Laboratoire de Production Microtechnique, CH-1015, Lausanne, Switzerland  
(Dated: April 14, 2024)

Assessing the effective relevance of multiband effects in the fullerenes is of fundamental importance to understand the complex superconducting and transport properties of these compounds. In this paper we investigate in particular the role of the multiband effects on the electron-phonon (el-ph) properties of the  $t_{1u}$  bands coupled with the Jahn-Teller intra-molecular  $H_g$  vibrational modes in the  $C_{60}$  compounds. We show that, assuming perfect degeneracy of the electronic bands, vertex diagrams arising from the breakdown of the adiabatic hypothesis, are one order of magnitude smaller than the non-crossing terms usually retained in the Migdal-Eliashberg (ME) theory. These results permit to understand the robustness on ME theory found by numerical calculations. The effects of the non degeneracy of the  $t_{1u}$  in realistic systems are also analyzed. Using a tight-binding model we show that the el-ph interaction is mainly dominated by interband scattering within a single electronic band. Our results question the reliability of a degenerate band modeling and show the importance of these combined effects in the  $A_3C_{60}$  family.

PACS numbers: 74.70.Wz, 63.20.Kr, 74.25.Kc

Although there is a large consensus about the phonon-mediated nature of the superconducting coupling in fullerenes  $A_3C_{60}$  compounds, the precise identification of the origin of so high critical temperatures ( $T_c$  up to  $\sim 40$  K) is still object of debate. Electron and phonon properties in these compounds are described in terms of molecular crystals, where the small hopping integral  $t$  between nearest neighbor  $C_{60}$  molecular orbitals sets the scale of the electronic kinetic energy, while electron-phonon coupling is essentially dominated by the intra-molecular vibrational modes [1]. First-principle calculations suggest that el-ph coupling is mainly dominated by the  $H_g$  modes, having energies  $\epsilon_{H_g} \sim 30 - 200$  meV, with some small contribution from the  $A_g$  modes. A simple application of the conventional Migdal-Eliashberg theory in these materials is however questioned for different reasons. On one hand, the small value of  $t$  gives rise to strong electronic correlation effects since  $t$  appears to be of the same order of the intra-molecular Hubbard repulsion  $U$  [1]. On the other hand, nonadiabatic effects are also expected to be relevant since the electronic energy scale  $t$  is of the same order as well of the phonon frequency scale  $\omega_{ph}$  [2]. In addition, the multiband nature of the electronic states  $t_{1u}$  involved in the pairing and the Jahn-Teller nature of the  $H_g$  phonon modes make the problem even more complex but also more interesting.

A popular tool to investigate el-ph properties in systems where all the energy scales  $t, U, \omega_{ph}$  are of similar order of magnitude, is the Dynamical Mean Field Theory (DMFT) [3] which does not rely on any small parameter expansion. In DMFT the lattice Hamiltonian is mapped in a local impurity model where the electron dynamics through the crystal is taken into account by a set (in multiband systems) of frequency-dependent Weiss fields.

This approach is particularly suitable in fullerenes because the intra-molecular el-ph interaction, just as the Hubbard repulsion, is local by construction when expressed in the basis of molecular orbitals. In order to provide a close set of equations, the hopping integrals  $t_{ij}^{n,m}$  are often chosen to be diagonal with respect to the indexes of molecular orbitals  $m, m'$ , and, in the absence of crystal field splitting, degenerate  $t_{ij}^{n,m} = \delta_{m,m'} t_{ij}$ . By using this approximation, the interplay between electronic correlation and el-ph coupling mediated by Jahn-Teller mode has been studied, and a reduction of the effective superconducting pairing for small  $U$  [4] accompanied by a remarkable enhancement of it close to the metal-insulator [5] transition has been found. Within the same approximation the validity of ME theory for a multiband Jahn-Teller ( $t \sim H$ ) model has also been investigated, showing a good agreement between ME theory and DMFT results up to intermediate-large values of the el-ph coupling  $\lambda < 1$ , in contrast to the case of a single band system interacting with a non Jahn-Teller mode (a  $A_g$ ) where ME theory breaks down for  $\lambda > 0.5$  [4]. The numerical solution of DMFT equations makes hard however to identify the physical origin of these results.

Aim of this paper is to provide an analytical insight about the relevance of the multiband and Jahn-Teller-like effects on the el-ph interaction in fullerenes. In particular we show that, assuming degenerate electronic bands, the peculiar symmetry of the Jahn-Teller  $H_g$  modes of the  $C_{60}$  molecules gives rise to a drastic suppression of the el-ph scattering channels described by vertex diagrams, enforcing the non-crossing approximation (NCA) which is at the basis of ME theory. Such a suppression is even more strict in a two band  $e_g$  model where vertex diagrams exactly cancel out. At the same time, we show that these results strongly depend on the de-

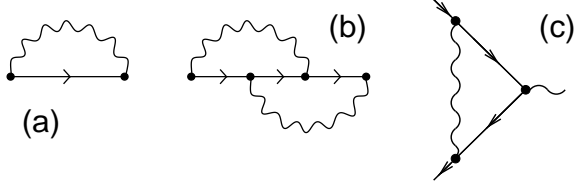


FIG. 1: Skeleton diagrams for: (a) el-ph self-energy in non-crossing approximation (ME); (b) lowest order expansion of the el-ph vertex function. Solid lines are electron Green's functions, wavy lines are phonon propagators, and small filled circles the el-ph Jahn-Teller matrix elements. Each pictorial element is a matrix in the space of the orbital molecular index. The same diagrammatic expressions hold true even in the superconducting state in terms of Nambu representation.

generate band assumption, whereas a careful analysis of the electronic structure of the  $A_3C_{60}$  compounds points out that the effective non-degeneracy of the  $t_{1u}$  bands significantly reduces the multiband Jahn-Teller effects.

The simplest way to consider multiband Jahn-Teller effects in fullerenes is to consider electrons in a tight-binding model on a fcc lattice interacting with a single  $\nu$ -degenerate  $H_g$  phonon mode with frequency  $\omega_0$ . The Hamiltonian reads thus:

$$H^{JT} = \sum_{m,m'=1}^3 \sum_{ij} t_{ij}^{m,m'} c_{im}^\dagger c_{jm} + \omega_0 \sum_i a_i^\dagger a_i + \frac{g}{10} \sum_{m,m'=1}^3 \sum_i V_{m,m'} c_{im}^\dagger c_{im} (a_i + a_i^\dagger) \quad (1)$$

where  $m, m'$  are indexes of the molecular orbitals,  $i$  is the site index and labels the  $\nu$ -degenerate vibrational modes.  $c$  ( $c^\dagger$ ) and  $a$  ( $a^\dagger$ ) are the usual creation (annihilation) operators for electron and phonon with the quantum number specified in the Hamiltonian, and the matrices  $V_{m,m'}$  are reported in literature [6]. This model will be compared in the following with a single band non Jahn-Teller model defined as:

$$H^0 = \sum_{ij} t_{ij} c_i^\dagger c_j + \omega_0 \sum_i a_i^\dagger a_i + g \sum_i c_i^\dagger c_i (a_i + a_i^\dagger) \quad (2)$$

The prefactor  $1/10$  in the el-ph scattering term of Eq. (1) has been introduced in order to normalize the effective coupling with Eq. (2), namely:

$$\frac{g^2}{10} \hat{V} \hat{V} = g^2 \hat{I} \quad (3)$$

Let us consider for the moment the case of diagonal and degenerate hopping integrals  $t_{ij}^{m,m'} = \delta_{m,m'} t_{ij}$ , as it is usually done in DMFT. In this case the molecular orbital index  $m$  represents a good quantum number also for the

Bloch-like electron bands, which remain degenerate, and both electron Green's function  $\hat{G}$  and its self-energy  $\hat{\Sigma}$  act thus as the identity matrix  $\hat{I}$  in the molecular orbital index  $\hat{G} = G \hat{I}$ ,  $\hat{\Sigma} = \Sigma \hat{I}$ . The el-ph matrix interaction at the ME level (Fig. 1a) can be evaluated in the  $m$ - $m'$  (3-3) multiband space, and it reads thus:

$$\hat{\Sigma}_{ME} = \frac{0}{10} \begin{pmatrix} 4 & 3 & 3 \\ 3 & 4 & 3 \\ 3 & 3 & 4 \end{pmatrix} \quad (4)$$

where  $\rho_0 = 2g^2 N(0) = \rho_0$  is the single degenerate contribution from intraband and interband scattering and  $N(0)$  is the electron density of states (DOS) for a single band of the three-degenerate model. The effective el-ph coupling in the normal state self-energy and in the Cooper channels are respectively given by  $\frac{m}{Z} = \frac{m_0}{m_0} = \rho_0$  and by the maximum eigenvalue of the matrix (4)  $\Sigma_{SC} = \max_{\text{eig}}[\hat{\Sigma}] = \rho_0$  [7], just as in the simple single band analysis. As a matter of fact, it is easy to see that the matrix (4) can take a block diagonal form and it behaves as a non Jahn-Teller single band system with effective el-ph coupling  $\rho_{\text{eff}} = \rho_0$  in the one-dimensional symmetric subspace  $\mathcal{C} = \frac{1}{\sqrt{3}} \sum_m c_m^\dagger |i\rangle$ . Note however that some residual el-ph scattering with coupling  $\rho_0 = 10$  is still operative in the orthogonal non-symmetric space in the molecular orbital index, although it has no contribution at the ME level if the band degeneracy is preserved. As we are going to see, this small component with el-ph coupling  $\rho_0 = 10$  is the only contribution surviving in the higher order terms which involve vertex diagrams beyond ME theory.

We discuss now the robustness of the ME theory with respect to the inclusion of highest order diagrams, i.e. vertex corrections, which are not taken into account in the ME framework. These diagrams are usually neglected in the ME theory for single band systems by virtue of the so-called Migdal's theorem which states that el-ph interaction processes containing vertex diagrams, as in Fig. 1b, scale with the adiabatic parameter  $\omega_0 = t$  and are thus negligible in conventional materials where  $\omega_0 = t \ll 1$  [8]. This results does not apply a priori however in the case of  $C_{60}$  compounds and of other narrow band systems where  $\omega_0 \sim t$  [9], so that the agreement between numerical DMFT data and ME theory remains somehow surprising. As we are going to show, the physical origin of such agreement stems from the particular matrix structure of the  $\hat{V}$  matrices in the Jahn-Teller multiband case of the fullerenes which leads to an almost complete cancellation of the vertex diagrams independently of the value of the adiabatic parameter  $\omega_0 = t$ .

Once more, the simplest way to understand this feature is to assume a diagonal-degenerate hopping term. In order to clarify the role of multiband Jahn-Teller effects on the vertex processes, let us compare at the skeleton level, for both tight H and a tight A models, a self-energy contribution involving a vertex diagram (Fig. 1b) and

a typical vertex-free diagram which is usually taken into account in ME theory (Fig. 1a). For a Jahn-Teller model we can write in a compact form:

$$G_a^0(k) = g^2 \sum_p^X D(k-p) G(p); \quad (5)$$

$$G_b^0(k) = g^4 \sum_p^X D(k-p) G(p) (p;k); \quad (6)$$

where  $p$  is the momentum-frequency vector  $(p; \omega_p)$  and  $\omega_p = \omega_p + \omega_k = 2\omega_k$ , and where  $(p;k)$  represents the lowest order vertex correction depicted in Fig. 1c. In the early 60's Migdal was able to show that

$$\lim_{\omega_0 \rightarrow 0} (p;k) / \frac{\omega_0}{t} = 0; \quad (7)$$

which allows to neglect vertex diagrams in the adiabatic limit  $\omega_0 \rightarrow 0$ .

The same diagrammatic picture (Fig. 1) and similar analytical expressions hold true for the multiband Jahn-Teller Hamiltonian model, properly generalized in the matrixial space of the molecular orbital index. For the diagonal-degenerate hopping term case the electron Green's function are once more proportional to the identity matrix  $\hat{I}$ , so that the only matrixial structure comes from the  $\hat{V}$  matrices in the elph scattering term. In explicit way we can write:

$$\begin{aligned} G_a^{JT}(k) &= \frac{g^2}{10} \sum_p^X \hat{V} \hat{V} \sum_p^X D(k-p) G(p) \\ &= g^2 \hat{I} \sum_p^X D(k-p) G(p); \end{aligned} \quad (8)$$

$$\begin{aligned} G_b^{JT}(k) &= \frac{g^4}{100} \sum_p^X \hat{V} \hat{V} \hat{V} \hat{V} \sum_p^X D(k-p) G(p) (p;k) \\ &= \frac{g^4}{10} \hat{I} \sum_p^X D(k-p) G(p) (p;k); \end{aligned} \quad (9)$$

where the last relation comes from the matrixial properties of the  $\hat{V}$  terms:  $[\hat{V} \hat{V} \hat{V} \hat{V}] = 100 = \hat{I} = 10$ .

The comparison between Eqs. (5)-(6) and Eqs. (8)-(9) shows that a strong reduction of the vertex diagrams, of a factor 10, is operative in the Jahn-Teller model appropriate for fullerides compounds in the case of a diagonal-degenerate hopping term, validating at a large extent the non-crossing approximation well beyond the adiabatic regime. We would like to stress that the robustness of the ME theory with respect to the inclusion of vertex diagrams does not stem from the negligibility of the vertex function, which can be well sizable for  $\omega_0 \rightarrow 0$ , but from the non commutativity of the  $\hat{V}$  matrices and from the assumption of diagonal and degenerate hopping term. As a matter of fact, these results hold true even if

the assumption of a diagonal hopping term is relaxed as long as the three electronic bands are degenerate. To show this, we can diagonalize the hopping term in Eq. (1) by the transformation:

$$C_a(k) = \sum_{i,m} M_k^{am} C_{i,m} e^{ik \cdot R_i}; \quad (10)$$

so that the elph scattering term becomes:

$$g \hat{V} \rightarrow \hat{G}_{k;k+q} = g \hat{U}_{k;k+q} = \hat{M}_k^{-1} \hat{V} \hat{M}_{k+q}^{-1}; \quad (11)$$

Since the electron Green's functions are still diagonal and degenerate  $\hat{G}(k) = \hat{I} G(k)$  in this new basis, the matrixial structure of the self-energy term is still only given by the elph matrices  $\hat{U}$ . We have thus

$$\begin{aligned} & \frac{1}{100} \hat{U} \hat{U} \hat{U} \hat{U} \\ &= \frac{1}{100} \hat{M}^{-1} \hat{V} \hat{M} \hat{M}^{-1} \hat{V} \hat{M} \hat{M}^{-1} \hat{V} \hat{M} \hat{M}^{-1} \hat{V} \hat{M} \\ &= \frac{1}{100} \hat{M}^{-1} \hat{V} \hat{V} \hat{V} \hat{V} \hat{M} = \frac{1}{10} \hat{I}; \end{aligned} \quad (12)$$

Finally, it is easy to check that, if the double-degenerate Jahn-Teller electron model is considered, the non-commutativity of the corresponding  $\hat{V}$  matrices leads to a complete cancellation of the vertex diagrams.

From the above discussion, one could be tempted to conclude that an effective non-crossing ME theory is expected to be enforced in fullerides due to an almost complete cancellation of the vertex processes. However, it should be stressed the above results are valid as long as the electronic bands can be considered degenerate. In the last part of this paper, we are going to argue that this latter assumption is not appropriate in  $A_3C_{60}$  compounds in regards with elph properties, and a single band model, which is unaffected by Jahn-Teller effects, is a better starting point for  $\omega_0 \rightarrow 0$ . In order to introduce a more realistic electronic band structure than a simple diagonal-degenerate model in the molecular orbital space, we consider a tight-binding (TB) model for the  $t_{1u}$  bands as discussed in Ref. [10] which reproduces first-principle LDA calculations with a high degree of precision. For sake of simplicity we consider the one-directional TB model where all the  $C_{60}$  molecules have a fixed orientation in the fcc crystal. Different directional ordering will be discussed in a more extended publication but they are not expected to qualitatively affect our results since they still predict a set of narrow bands with only few Fermi cuts. The electronic hopping term in Eq. (1) is then diagonalized by the  $\hat{M}$  matrix introduced in (10), where each matrix element depends on the electronic momentum  $k$ . For a generic point of view, the degeneracy of the electronic states in the crystal structure is preserved only on special high-symmetry points. The electronic band structure along the high-symmetry axes

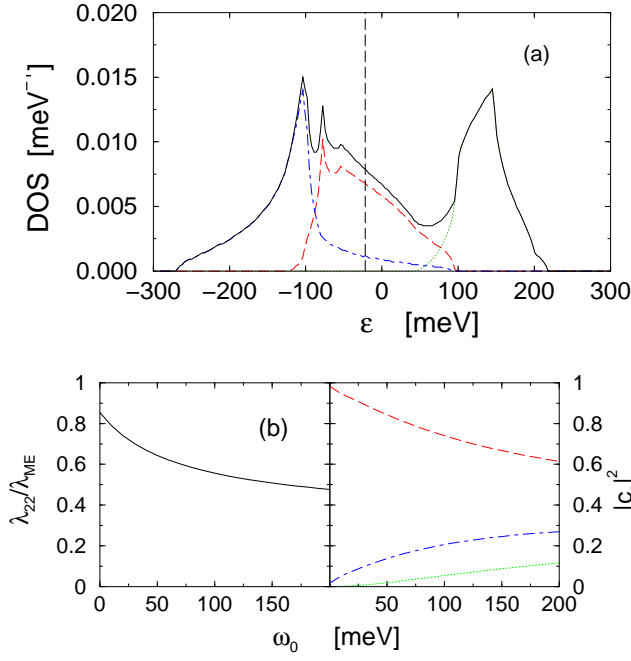


FIG. 2: (color online). (a) Total DOS (black solid line) and partial DOS for each electronic band in the one-directional TB model for  $A_3C_{60}$ . The dashed vertical line represents the Fermi level. (b) Left panel: Ratio between the only intraband contribution  $\lambda_{22}$  and the total el-ph coupling  $\lambda_{\text{ME}}$ . Right panel: band components  $|c_a|$  of the eigenvector of the multiband el-ph coupling matrix  $\hat{\lambda}$ .

of the fcc Brillouin zone and the total electron DOS has been widely reported in literature [1]. In order to assess to which extent the realistic band structure can be approximated by a degenerate three-band model, it should be noted that (low energy) electronic and transport properties are mainly determined by quantities defined at the Fermi level, as the Fermi surface itself, the electron DOS at the Fermi level, the Fermi velocity, etc. A realistic band structure can thus be modeled as a degenerate three-band system only if it presents qualitatively similar Fermi sheets, with similar densities of states and similar Fermi velocities. In this perspective  $A_3C_{60}$  compounds seem not to be a good candidate since it is known to have only two Fermi cuts of the electronic bands with quite different Fermi surfaces [11]. The smooth topological evolution of the Fermi surfaces with the Fermi level permits to identify in an unambiguous way, for what concerns electronic and transport properties, the three electronic bands with their corresponding DOS. The electronic DOS for each band, as well as the total DOS, is plotted in Fig. 2a, which shows that the electronic band structure is largely dominated at the Fermi level  $\epsilon_F = -23$  meV, by a single band which is roughly half-filled, with two additional bands which are quite far from the Fermi level. Only two bands have finite DOS at the Fermi level, in agreement with the report of only two Fermi surface.

We would like to stress that the non-degeneracy of the DOS is not related to the removing of the crystal field symmetry, but it is uniquely determined by non degeneracy of the electronic dispersion. If we evaluated the mean value  $\bar{\epsilon} = \langle \epsilon \rangle$  and the variance  $\sigma^2 = \langle \epsilon^2 \rangle - \bar{\epsilon}^2$  of each band, we obtain  $\bar{\epsilon}_1 = -120$  meV,  $\sigma_1 = 60$  meV,  $\bar{\epsilon}_2 = -23$  meV,  $\sigma_2 = 47$  meV,  $\bar{\epsilon}_3 = 135$  meV,  $\sigma_3 = 30$  meV. These considerations suggest  $A_3C_{60}$  can be modeled in good approximation as a single band system and that multiband effects are qualitatively irrelevant as far as the phonon energy is not sufficiently high to switch on el-ph scattering between different bands.

We sustain this intuitive argumentations with a numerical calculation of the multiband el-ph matrix interaction  $\hat{\lambda}_k$  within the non-crossing approximation (Fig. 1a) which generalizes the ME theory to systems with generic DOS  $N(\epsilon)$ . For sake of simplicity we consider unrenormalized electron and phonon propagators, with energy spectra respectively given by the TB electron dispersion and by the phonon frequency  $\omega_0$ . A  $k$ -independent el-ph interaction is obtained in the usual way by a proper average over the Fermi surface:  $\lambda^{ab} = \frac{1}{N_F} \sum_k D_k^{(a)} D_k^{(b)} = \frac{1}{N_F} \sum_k D_k^{(a)} D_k^{(b)}$ , where  $D_k^{(a)} = (1 - \eta_k) \omega_0^{-1/2} \langle c_k^\dagger c_k \rangle$ , which reduces to  $\lambda^{ab} = \frac{1}{N_F} \sum_k D_k^{(a)} D_k^{(b)}$  for  $\omega_0 \rightarrow 0$ . For sake of simplicity we neglect self-energy effects, which are expected to shrink furthermore the electron bands at the Fermi level. In order to provide a first simple estimate of multiband effects, in the left panel of Fig. 2b we compare the effective total el-ph coupling  $\lambda_{\text{ME}}$ , obtained as the maximum eigenvalue of the matrix  $\hat{\lambda}$ , with the single intraband contribution  $\lambda_{22}$  relative to the high DOS central band shown in Fig. 2a. For  $\omega_0 \rightarrow 0$ ,  $\lambda_{22} = \lambda_{\text{ME}} \approx 0.86$ , pointing out that the dominant el-ph scattering comes from intraband processes with a small interband contribution due to the small DOS of the lowest electron band. As expected the discrepancy between  $\lambda_{22}$  and  $\lambda_{\text{ME}}$  becomes more relevant as the activation of high energy interband processes by the phonon increases. To quantify further the role of multiband effects we plot in the right panel of Fig. 2b the components of the eigenstate of the el-ph scattering matrix on the Bloch-like band index  $a$ . For  $\omega_0 \rightarrow 0$  only the  $j_2$  component is sizable reflecting that el-ph scattering is mainly intraband. By increasing  $\omega_0$  interband processes are gradually turned on, but, for the physical range of  $\omega_0 < 200$  meV, intraband el-ph scattering within the central band are still dominant. In the opposite limit  $\omega_0 \rightarrow \infty$  (where  $\omega_0$  being the total electronic bandwidth) the three components become identical and the  $A_3C_{60}$  compounds are expected to behave as a degenerate three band system.

In conclusion, in this paper we have investigated the role of the electronic structure on the multiband Jahn-Teller effects in the el-ph interaction in fullerides compounds. We found that a band degenerate model leads to an almost cancellation of vertex diagrams enforcing the validity of ME theory, as observed by Quantum Monte

Carb DMFT data. On the other hand, we also show that realistic band structure calculations suggests that the el-ph interaction in  $A_3C_{60}$  compounds is mainly dominated by intraband scattering within a single band. Note that similar conclusions are not expected to apply for electron-electron (Hubbard) interaction where relevant scattering processes are not restricted in an energy window around the Fermi level. Note also that electronic and vibrational disorder could in principle strongly mix intra- and inter-band el-ph scattering.

The effective role of the non degeneracy on the metal-insulator transition driven by the Hubbard repulsion and the inclusion of possible crystal splittings and disorder will be the future developments of the present work.

We thank M. Capone and N. Manini for fruitful discussions and the careful reading of the manuscript. This

work was partially funded by the INFN project PRA-UMBRA and by the MIUR project FIRB RBAU017S8R.

- 
- [1] O. Gunnarsson, *Rev. Mod. Phys.* **69**, 575 (1997).
  - [2] E. Cappelluti et al, *Phys. Rev. Lett.* **85**, 4771 (2000).
  - [3] A. Georges et al, *Rev. Mod. Phys.* **68**, 13 (1996).
  - [4] J.E. Han et al, *Phys. Rev. Lett.* **90**, 167006 (2003).
  - [5] M. Capone et al, *Science* **296**, 2364 (2002).
  - [6] J.E. Han et al, *Phys. Rev. B* **60**, 6495 (1999).
  - [7] H. Suh et al, *Phys. Rev. Lett* **3**, 552 (1959).
  - [8] A.B. Migdal, *Sov. Phys. JETP* **7**, 996 (1958).
  - [9] C. Grimaldi et al, *Phys. Rev. Lett.* **75**, 1158 (1995).
  - [10] S. Satpathy et al, *Phys. Rev. B* **46**, 1773 (1992).
  - [11] S.C. Erwin and W.E. Pickett, *Science* **254**, 842 (1991).